10-19-2012

An imaging neutron/gamma-ray spectrometer

James M. Ryan
University of New Hampshire, James.Ryan@unh.edu

Chris Bancroft
University of New Hampshire

Peter F. Bloser
University of New Hampshire, Peter.Bloser@unh.edu

Dominique Fourguette
Michigan Aerospace Corp.

Liane Larocque
Michigan Aerospace Corp.

See next page for additional authors

Recommended Citation

James M. Ryan ; Christopher Bancroft ; Peter Bloser ; Dominique Fourguette ; Liane Larocque ; Jason Legere ; Amanda Madden ; Mark L. McConnell ; Jane Pavlich ; Greg Ritter ; Greg Wassick and Marissa Rousseau " An imaging neutron/gamma-ray spectrometer ", Proc. SPIE 8509, Penetrating Radiation Systems and Applications XIII, 850905 (October 19, 2012); doi:10.1117/12.930048; http://dx.doi.org/10.1117/12.930048

Authors

James M. Ryan, Chris Bancroft, Peter F. Bloser, Dominique Fourguette, Liane Larocque, Jason S. Legere, Amanda C. Madden, Mark L. McConnell, Jane Pavlich, Greg Ritter, Greg Wassick, and Marissa Rouseau

An Imaging Neutron/Gamma-Ray Spectrometer

James M. Ryan[a], Christopher Bancroft[a], Peter Bloser[a], Dominique Fourguette[b], Liane Larocque[b], Jason Legere[a], Amanda Madden[a], Mark L. McConnell[a], Jane Pavlich[b], Greg Ritter[b], Greg Wassick[b], Marissa Rousseau[a]

[a]Space Science Center, University of New Hampshire, 8 College Rd., Durham, NH USA 03824;
[b]Michigan Aerospace Corp., 1777 Highland Drive, Suite B, Ann Arbor, MI USA 48108

ABSTRACT

We present the design and development of a dual-species, neutron/γ-ray imaging spectrometer for the identification and location of radioactive and special nuclear materials (SNM). Real-time detection and identification is important for locating fissile materials. These materials, specifically uranium and plutonium, emit neutrons and γ rays via spontaneous or induced fission. Co-located neutron and γ-ray emissions are a sure sign of fissile material, requiring very few spatially correlated events for a significant detection. Our instrument design detects neutrons and γ rays from all sources in its field of view, constructs images of the emission pattern, and reports the spectra for both species. The detection principle is based upon multiple elastic neutron-proton scatters in organic scintillator for neutrons, and Compton scattering in organic scintillator followed by photoelectric absorption in inorganic scintillator for γ rays. The instrument is optimized for neutron imaging and spectroscopy in the 1-20 MeV range. We recorded images and spectra of a Cf-252 source from 0.5 - 10 MeV, and have done similarly for several γ-ray sources. We report the results of laboratory testing of this expanded instrument and compare them to detailed Monte Carlo simulations using Geant4.

Keywords: neutrons, gamma rays, imaging, spectroscopy

1. INTRODUCTION

Imaging brings new power to the problem of detecting, locating and identifying nuclear material—specifically γ emitters and/or fissile material. Neutrons and γ rays are, by their nature, resistant to detection, and defy easy imaging and spectroscopy. Neutron detection is often in the form of registering moderated or thermalized neutrons from a fast neutron source, thereby primarily detecting moderating material rather than the parent source. Furthermore, because one only measures the charged particles produced by a neutral interactions, deducing the properties of the parent source is ambiguous, besides being difficult.

Registering moderated neutrons or scattered γ rays yields degraded or little information about the incident direction or energy. Measuring fast neutrons or γ rays in a bulk detector provides a compromised energy measurement, but still lacks directional information. A double-scatter telescope corrects these deficiencies, but pays the penalties of increased complexity and low efficiency by requiring two neutron (or γ) scatters, but it benefits in the end because the elastic scatter kinematics can be used to constrain the incident velocity vector while simultaneously performing a quality energy measurement. The γ-ray version of this concept is a Compton telescope, a device that has seen extensive use in space for astrophysics research[1].

2. DETECTION TECHNIQUE

2.1 Detection Physics—neutrons

Neutrons have no charge, and therefore do not readily interact. Thus, they must be detected by indirect methods. A preferred method for neutron detection at MeV energies exploits the large elastic n-p scattering cross section. The choice material, serving the functions of neutron scatterer and recoil proton detector, is an organic scintillator. This material consists of mainly hydrogen and carbon, in the number ratio range of 1.0 to 2.0. The relative concentration of hydrogen varies with scintillator type.

To perform imaging, an incident neutron must undergo an n-p scatter in each of two detectors. One must be able to follow the path of the neutron once it enters the instrument, measuring the location, relative time and energy deposits of each n-p interaction. Consider the scenario shown in Fig. 1—a neutron, whose incident direction is unknown, as it undergoes two n-p scatters. By measuring the spatial coordinates of the two interaction sites and time of flight (ToF), one can determine the energy and direction (*i.e.*, momentum vector) of the scattered neutron. By measuring the energy of the

Penetrating Radiation Systems and Applications XIII, edited by Gary P. Grim, H. Bradford Barber, Proc. of SPIE Vol. 8509, 850905 · © 2012 SPIE · CCC code: 0277-786X/12/$18 · doi: 10.1117/12.930048

first recoil proton, one can then compute the energy of the incident neutron as well as its scatter angle. With this information one can constrain the incident neutron direction to lie on the mantle of a cone about the recoil neutron velocity vector (Fig. 1). The scatter angle is computed as $\sin^2 \theta = E_{p1}/E_n$. By projecting the cone onto an object plane or sphere, one creates an event circle (or ellipse) for each event, also shown in Fig. 1. From the intersection of multiple event circles, through statistical means it is possible to obtain an image of a neutron source. We assume that the detectors are thin to avoid multiple scatters.

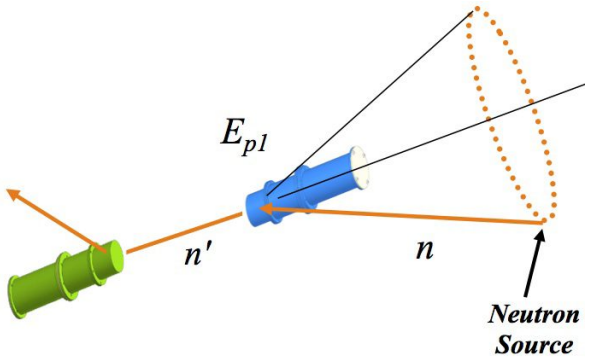

Fig. 1. Neutron double-scatter kinematics.

2.2 Detection physics—γ rays

The process is very similar for the case of γ rays. This basic principle has been employed extensively and successfully for γ-ray imaging in Compton telescopes to image the complex distribution of point and extended sources in the sky. What changes is that the scattering process is Compton scattering rather than hard-sphere scattering and the governing kinematic equation is the Compton equation, $\cos \theta = 1 - 0.511 (E_{\gamma'}^{-1} - E_{\gamma}^{-1})$, where energy is expressed in units of MeV. See Fig. 2. The other main difference is that the ToF measurement does not provide any energy information, but rather serves to help differentiate γ rays from sub-luminal particles. The scattered photon energy, $E_{\gamma'}$, is obtained from the interaction in the second detector. It follows that a quality energy measurement should be performed in the second detector, *i.e.*, full energy absorption and good energy resolution.

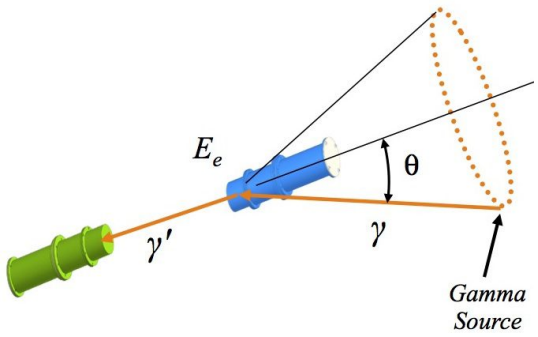

Fig. 2. Compton scatter diagram

In its most simple form, the imaging takes place by superposing event circles onto an image plane or the interior of sphere. Events where the energy is fully measured will have their event circles pass through the location or direction of the source. That point of intersection is broadened by the energy resolution effect of the detectors and by the finite size of the detector cells, *i.e.*, uncertainty in the axis of the cone. Incorrect measures of the recoil particle energy, whether it is a neutron (ToF measure) or a γ ray (E_2 measure), results in an incorrect half angle for the cone, broadening the area of the intersection point if near the optical axis. Systematic effects (*e.g.*, coma) arise as the source departs from the optical axis.

By selecting events that pass within some predetermined angle from a source (either known or detected), one can construct a spectrum of counts for which the energy of each particle is fully measured.

3. NSPECT

3.1 The Dual-species Detector Concept

Previous generations of neutron imaging telescopes have been constructed with either plastic or liquid scintillator. Liquid scintillator systems have the advantage of high hydrogen content, relatively good light output, and the ability to perform pulse shape discrimination. Pulse shape discrimination (and ToF) allows the system to reject γ rays, important for high γ background environments.

For γ rays, one needs a low-*Z* scattering material, such as an organic scintillator, preferably with pulse-shape discrimination. One also needs a high-density, high-*Z* calorimetric material for the second interaction. Both detecting materials must be fast—for background suppression for γ rays and energy measurement for neutrons.

The instrument, NSPECT—Neutron Spectroscope, is shown in Fig. 3. It is a three-layer system using three different scintillator materials. The front detector layer is made up of 1″ cylindrical cells of plastic scintillator, read out by fast, rugged 1″ photomultiplier tubes (PMT). The second or middle detector layer is comprised of 1″ stilbene scintillator cells read out by similar PMTs. Scatters between these two planes constitute the best measurement for neutrons. A time-of-flight measurement is made between these planes. All cells represent independent data channels. When a neutron interacts in the forward detector plane D1, analog signals from that detector plane are generated from the analog sum of all the cells in D1. Those signals initiate the ToF measurement, create a fast logic signal to test for time coincidence with any trigger in D2, and serve as an analog pulse height for the energy deposited by the neutron in D1. The cell identification is taken to be the interaction location, *i.e.*, a spatial resolution of 1″ corresponding to a particular cell. Multiple signals from different D1 cells will reject that event. Similar signal processing takes place in D2, where the sum signal stops the ToF measurement and the cell that triggers is identified and recorded.

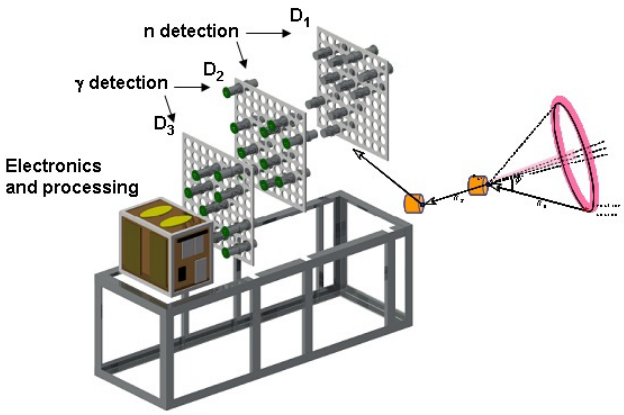

Fig. 3. Design schematic.

The signal from the stilbene in D2 can be used to identify whether the ionizing particle is either fast (electron, muon) or slow (proton or heavy ion). The two types of particles differ in their detailed pulse shape—a function of the chemistry of the scintillator. Neutron-initiated events can thus be identified and selected for further data analysis. Electron ionization pulse shapes when in coincidence with a D1 (*i.e.*, a γ ray between D1 and D2) signal can be utilized, but are generally discarded. A photograph of the instrument is shown in Fig. 4.

The two scintillator planes are separated by 37 cm, on center. A γ ray over this distance registers a 1.25-ns ToF, while a 1-MeV neutron requires ~30 ns to cover the same distance. Oblique trajectories yield longer ToF values, but this effect is corrected using the locations of the cell that triggered. The ToF range is of order 50 ns, extending above and below typical fast neutron speeds. By having a longer ToF range, one automatically obtains a measure of the accidental coincidence rate—in important measurement in intense radiation environments.

For the detection of γ rays, a third layer D3 is employed. It is of the same dimensions as the other layers in all respects, but the scintillator is bismuth germanate, BGO. It is separated from D2 by the same distance, *i.e.*, 37 cm. The registration

of the different planes and their orientations is controlled to better than 1 mm. The fact that no gas or liquid is used is a consideration for field use.

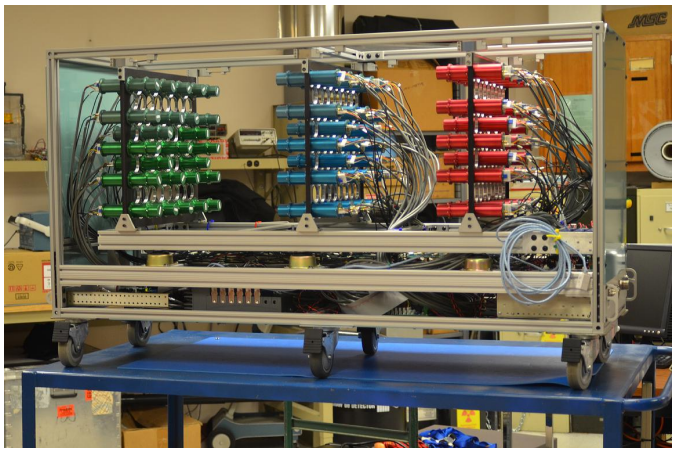

Fig. 4. The NSPECT instrument. D1 is at the left.

The majority of good γ-ray scatters occurs between D2 and D3. The pulse-shape signal in the D2 stilbene detectors for the detection of γ rays is then used to choose γ events rather than reject them. Photon events between D1 and D3 are also recorded, but are fewer in number because of the extra separation. No pulse-shape information is available from D1. The final acceptance ToF window for γ rays is of order 5 ns. All combinations of plane coincidences are recorded, later to be sorted for event type for analysis either as γ rays or neutrons.

The instrument is designed to operate eight hours on battery power with each plane populated with seventy-seven detector cells. Analog data are processed in an on-board computer, digitized and formatted for transmission to a remote computer for real-time monitoring or analysis and/or data archiving. The connection between the on-board and remote computers can be by ethernet cable or wireless communications.

The instrument is controlled through the remote computer, nominally a laptop computer running Lab View™. The remote computer currently monitors HV, but can accommodate other housekeeping parameters, such as temperature, voltages, count rates in all detector cells and other rates, important for assessing instrument behavior and performance. The detector cell planes are sprung to absorb shock during transit.

3.2 The NSPECT System

At the time of this writing, each plane is populated with twenty-five cells. Each plane is separated from its neighbor by 37 cm. The cells are screw mounted in a precision aluminum frame to maintain precise registration. The aluminum structure is shock mounted in a chassis that also houses the supporting signal processing electronics, power systems and on-board computer. The control, monitoring and imaging computer is remotely located and communicates with the on-board computer. The full system, exclusive of the remote computer operates on ~20 W.

As seen in Fig. 5, the planes are square in cross section and about ⅓ populated. The cells within each plane are spaced identically, *i.e.*, approximately with uniform spacing between the cells of each plane. The outer dimensions of the instrument are: length, 1.2 m; height, 0.9 m and width, 0.8 m. Supporting electronics sit below the detecting system, thus the taller height dimension. As discussed below, because of the 1-m scale of the instrument, parallax effects arise in imaging sources nearer than about 2 m from D1. Is such cases, knowledge of the source distance is required for proper focusing of the optics.

All cells were gain matched via HV adjustments, but finer scale gain matching takes place using calibration sources and is handled in the data processing. The ToF system, between D1 and D2, is normalized to the central cell in each plane and can be periodically checked with a centrally located ^{60}Co source. The ToF adjustments for the D3 plane are much less critical, because of the intrinsically poorer ToF resolution of BGO.

The functioning system has been exposed to ^{252}Cf sources and several γ-ray sources, the results of which are discussed in Sec. IV.

After exposing the instrument to a source of unknown nature, double scatters in each data run are first sorted using hardware coincidence criteria. For example, coincidences between D1 and D2 are assumed to be neutron events, whereas coincidences between D2 and D3 are assumed to be γ events. Signals from D1 and D2 must occur within 50 ns of each other to satisfy the low-level coincidence requirements and pulse height thresholds were set to 50 keV_{ee} (electron equivalent). The data processing of the D1 and D2 cells is the most complicated, because of the importance of the ToF measure for neutron events. Corrections in each plane for systematic electronic timing offsets (*e.g.*, cable length and first-dynode transit time) and walk. The ToF measure for each recorded event is then normalized to 37 cm. The pulse-shape parameter is walk-corrected to allow for easier selection of either proton- or electron-produced signals.

Neutron events at this point can be selected by requiring a ToF measure greater than that of photons and a proton-induced pulse shape in D2.

Cuts on ToF and pulse shape are made in software. Established neutron time-of-flight and pulse shape discrimination parameters can be adjusted to expand or contract the data acceptance window for subsequent analysis.

After data selections, count spectra can be constructed as well as images, using the appropriate scattering kinematics. De-convolving the neutron or photon energy spectra requires additional algorithmic processing using the instrument response, either computer generated or measured. More advanced image processing can be exercised too, as opposed to simple event circle overlaps. The non-linear pulse height output of the organic scintillators to the saturated ionization produced by protons is taken into account.

3.3 Characterizing the system

3.3.1 Imaging Capabilities

The factors that determine the ultimate imaging quality are the accuracy and precision of the scatter-angle measurement and the spatial-location uncertainty in the scattering sites. The net effect is quantified in the so-called ARM distribution (Angular Resolution Measure). The ARM quantity is the difference between the kinematically measured scattering angle (from energy and ToF) and the geometric scattering angle (knowing the true source position). The ARM distribution in Fig. 5 was obtained in a well controlled two-cell experiment. Gain and ToF calibrations and matching complicate multi-cell measurements of this quantity. The width of this distribution reflects the net uncertainties produced by the spatial, energy and ToF uncertainties and is of order 10˚ FWHM (full width half-maximum) for both neutrons and γ rays. Any skewness of this distribution represents the effect of systematic errors.

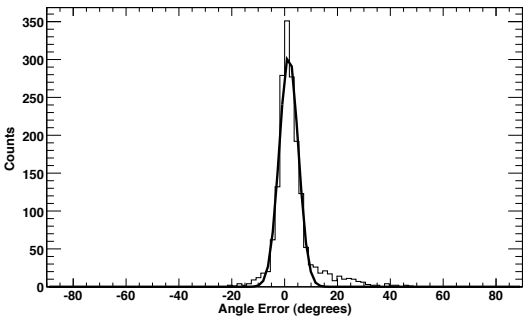

Fig. 5. The ARM distribution of a two-module experiment.

3.3.2 Spectral Capabilities

To select neutrons that are fully measured, we choose events that fall within ±20˚ of 0˚, the mean of the ARM distribution and use them for spectral analysis. These are events that satisfy neutron-proton elastic scattering kinematics over the known trajectory. The neutron count spectrum is then constructed on an event-by-event basis; the total neutron energy is the sum of the recoil proton energy deposited in the first detector plus the energy of the scattered neutron determined from ToF. By selection, the energy measurement is accurate, broadened only by the instrument resolution with little skewness.

Similar steps produce a γ-ray spectrum, *i.e.*, selecting events that pass within some pre-determined angle, typically 10˚, of a perceived or known source.

The neutron energy threshold of the NSPECT system is ~500 keV_{pe}. This threshold for the neutron double scatter measurement is driven by the light output of both D1 and D2 and their associated front end electronics (FEE).

4. PERFORMANCE OF THE PARTIALLY POPULATED INSTRUMENT

4.1 Fundamental parameters

After correcting for walk, first-dynode transit-time, cable length and geometrical separation, the net time-of-flight (D1 to D2) resolution is about 900 ps (Fig. 6) at 1 MeV_{ee}. The Angular Resolution Measure is about 9˚ for γ rays and 10˚ for neutrons. The γ-ray energy resolution is 19% at 662 keV, mostly determined by the resolution of BGO (discussed below). Because no monochromatic neutron source was available, we estimate (from D1 energy resolution and ToF resolution) a neutron energy resolution of 10%.

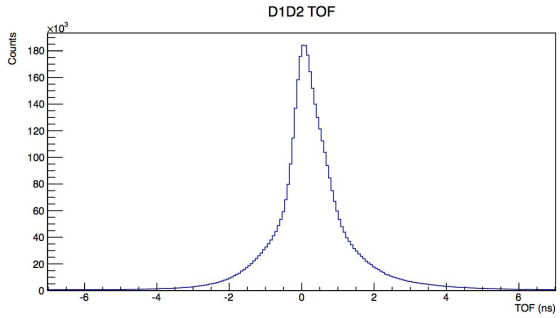

Fig. 6. Time-of-flight resolution between D1 and D2 using ^{60}Co γ rays.

4.2 Neutron Imaging and Spectroscopy

At a distance of 2 m from D1, we placed a ^{252}Cf source on the instrument optical axis. A distance of 2 m from D1 is enough to avoid significant parallax issues. We then moved the source 1 m orthogonally off axis (maintaining the same normal distance to D1 plane). The resulting images from these two exposures are shown in Fig. 7. The width of both images is about 35 cm, with the peak or centroid known to about 4 cm, depending on the statistics of the image. The count spectrum from both exposures is shown in Fig. 8 and has the Watt spectrum superposed. The spectrum was constructed by selecting event circles that pass within ±20˚ of the known source location—a so-called ARM cut. Two points to note: the first being that the instrument threshold in this configuration is about 1 MeV, catching the majority of the Watt spectrum; the second being that the resemblance of the count spectrum to the neutron intensity spectrum implies that the instrument response is largely diagonal and varies little from 1 MeV to 10 MeV. The diagonal nature of the response function means that the energy of a registered neutron is roughly that of the true neutron (with attendant broadening) with no skewness in the form of a "Compton-like" tail. We also note that the shape of the count spectrum varies little from on-axis to 27˚ off-axis.

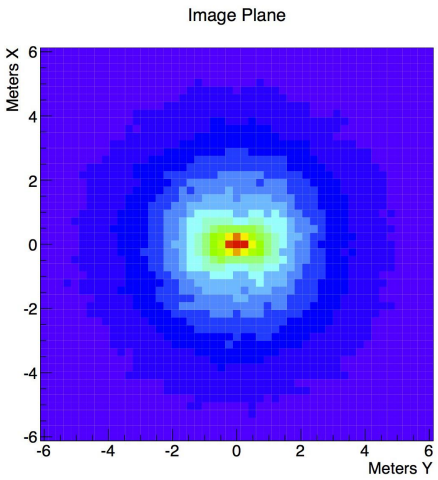

Fig. 7a. Neutron image of bare ^{252}Cf @ 2 m, on axis.

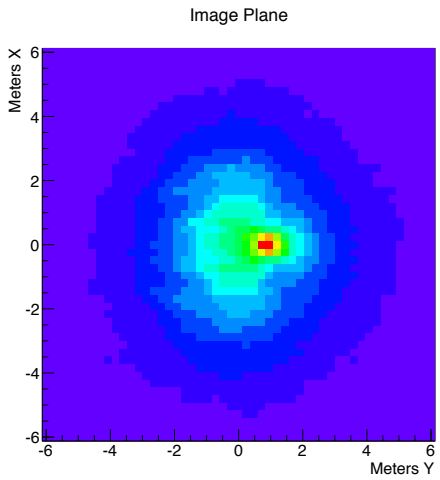

Fig. 7a. Neutron image of bare ^{252}Cf @ 2 m, 1 m off axis.

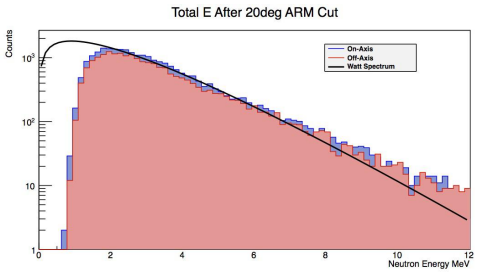

Fig. 8. ^{252}Cf count spectrum from on- and off-axis exposures.

4.3 γ-ray Imaging and Spectroscopy

We performed a similar test with a ^{137}Cs source, again with the source on axis and 1 m off axis at a normal distance of 2 m. The images and spectra from those exposures are shown in Figs. 9 and 10. As with the neutrons, the image size is about 35 cm, but the centroid is known much better. A spectrum was produced with a 12˚ ARM cut (Fig. 11). The peaks from the exposures on and off axis agree in peak energy to within 1%. The photopeak fraction is greater for the off-axis exposure, because less energy is required to be absorbed by D3 with the larger scatter angle. Thus, the photopeak amplitude is larger with respect to the already-small Compton tail. The imaging requirement suppresses the Compton tail. Photons that are only partially absorbed in D3 result in anomalously large scatter angle measures compared to the true scatter angle. The nature of the γ source is evident when such high quality spectra are collected, even with BGO quality resolution.

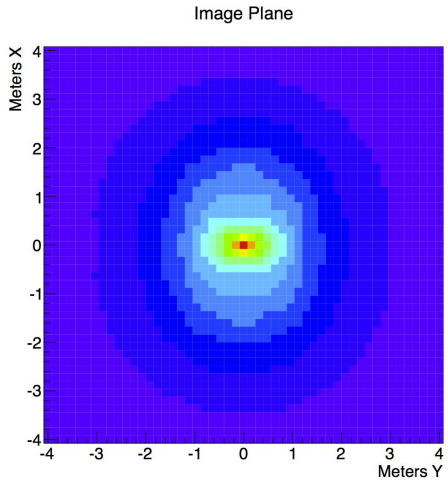

Fig. 9a. ^{137}Cs image @ 2 m, on axis.

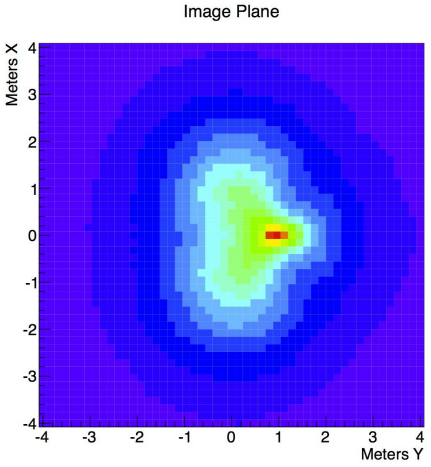

Fig. 9b. ^{137}Cs image @ 2 m, 1 m off axis.

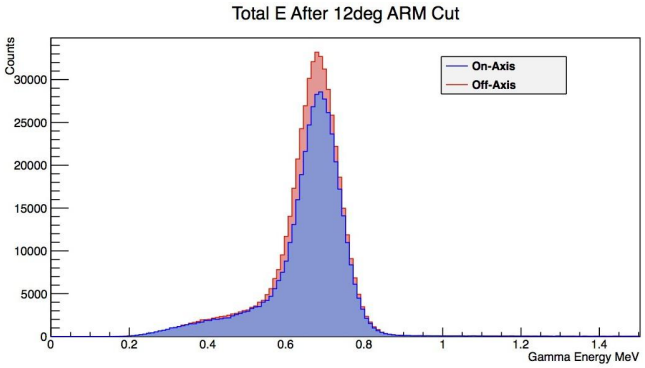

Fig. 10. ^{137}Cs spectrum using a 12˚ ARM cut

4.4 Multiple neutron sources

We wanted to test the system's ability to recognize multiple neutron sources in the field of view. With only one ^{252}Cf source available, two separate exposures were taken—one 1 m off axis to the left and the other 1 m off axis to the right. The two data files were then concatenated and processed as one. This process produces the same result except in the case where the two sources produce count rates too high for some aspect of the system. This was not the case here—the count rates from the individual data runs were a fraction of the maximum intensity the system would handle. This means that the net rate from two such sources does not result in any significant pulse pile up effects, either in the front end electronics, the processing window or the pulse-shape discrimination circuit. Furthermore, two such hypothetical sources would result in accidental coincides at a small fraction of the rate of true coincidences, so we feel justified in fabricating this exposure. Shown below (Fig. 11) is the dual-source image and (Fig. 12) the raw unselected count spectrum. The exposure times for the runs were equal, but short, compared to those in Fig. 8. The low statistics are evident. The color scale is auto-normalizing in the image.

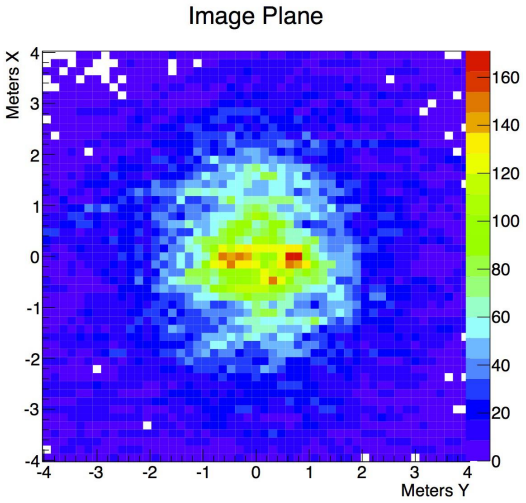

Fig. 11. The neutron image of two ^{252}Cf sources.

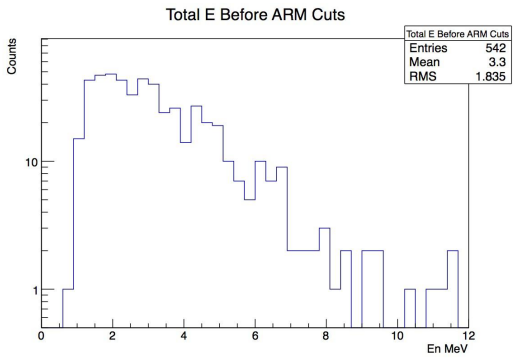

Fig. 12. The raw, unselected count spectrum from the exposures in Fig. 11.

With longer exposures and improved statistics we would expect the ghost image between and below the two real sources to vanish. We also note that the exponential Watt spectrum emerges with no special data selections or processing. This implies that a many-fragmented quantity of fissile material with no fragment producing a coherent image would still be recognized, because of a clear Watt-like count spectrum.

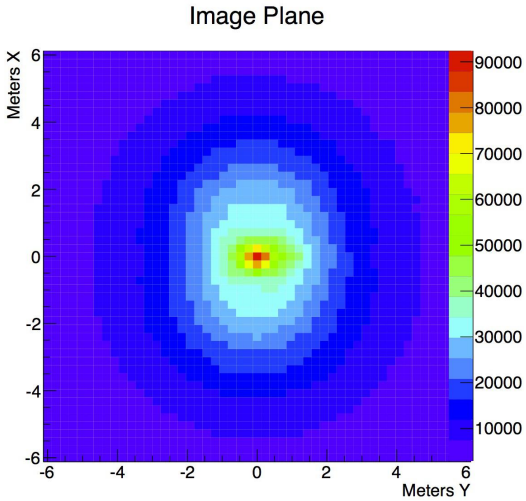

Fig. 13. The γ image of a ^{137}Cs on axis and a ^{252}Cf source 1 m off axis.

4.5 Mixed radiation sources in the field of view.

A potentially confounding situation is that of a neutron source in an intense γ field. This is the problem that drives the requirement for a typical neutron detector to have a gamma rejection ratio exceeding 10^6. To test this we put the ^{137}Cs source on axis with the ^{252}Cf source 1 m off axis at a normal distance from D1 of 2 m. Because of the intensity of the source and the high efficiency of NSPECT to register and detect γ rays, the γ signal is much greater that the neutron signal. The two sources were imaged and processed twice, first as a totally γ source(s) and then as a neutron source(s). The result of the γ imaging is shown in Fig. 13. Both sources are present through the γ filter, but because of the intense γ emission from the ^{137}Cs source, it overwhelms the γ image of the off-axis ^{252}Cf source.

We can be more critical by imposing energy filters on the γ image in Fig. 13. In Fig. 14, are the same γ data in a window around 662 keV, specifically 325-800 keV. The image is hardly distinguishable from that in Fig. 13. However, the complement energy window, *i.e.*, excluding the 325-800-keV window is shown in Fig. 15. The ^{252}Cf shows up clearly through its γ emission.

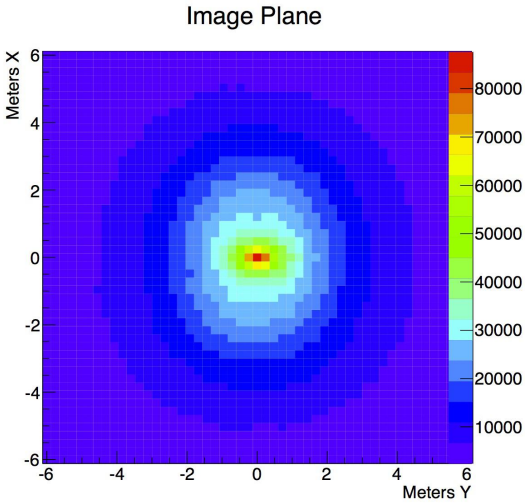

Fig. 14. The γ image in an energy window around 662 keV.

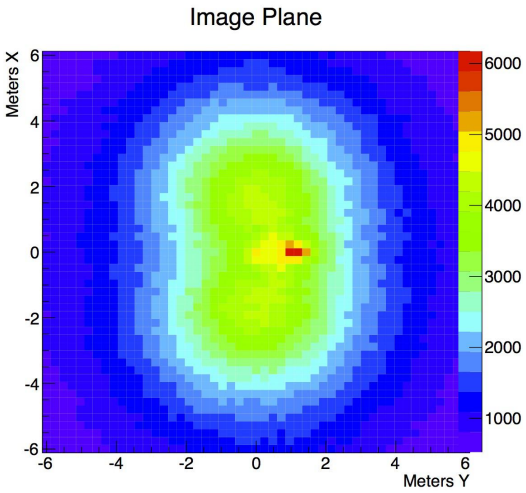

Fig. 15. The γ image excluding the energy window around 662 keV.

To test how this affects the neutron detection capability, we then ran the data through a neutron filter, the results of which are shown in Fig. 16. The maximum intensity in neutrons coincides with the ^{137}Cs-deselected γ image maximum. To verify that we are, indeed, seeing neutrons, the count spectrum of the events in and around the neutron image is shown in Fig. 17—the Watt spectrum is apparent.

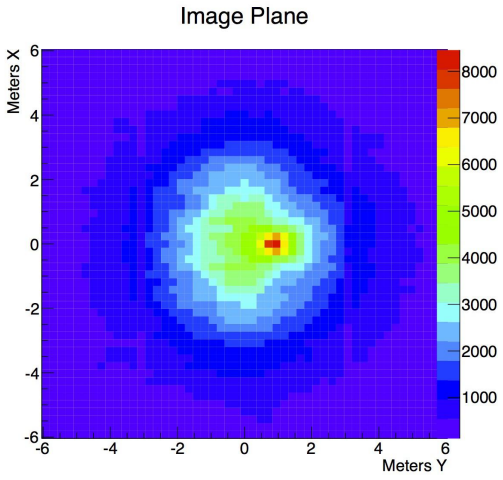

Fig. 16. The neutron image of the field of view of Fig. 13.

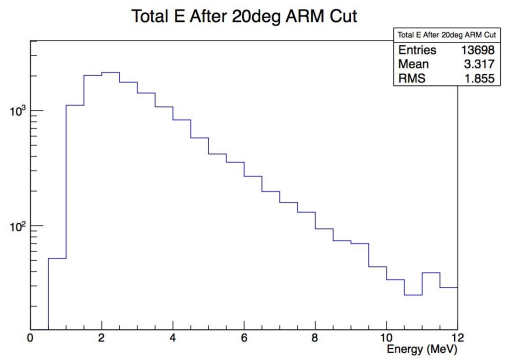

Fig. 17. The neutron spectrum from the region around the maximum neutron signal in Fig. 16.

4.6 Shielded Sources

One could expect under normal circumstances to encounter shielded sources, *i.e.*, fissile material embedded in a hydrogenous container to scatter and absorb neutrons. It is important to be able to recognize such configurations. To that end, we conducted short exposures of the instrument to bare and shielded sources. The shielding was in the form of a 30-cm ⌀ sphere of high density polyethylene (HDPE). Both neutron and γ-ray data were accumulated. Shown in Fig. 18 are the neutron and γ images of a bare ^{252}Cf source. The relatively strong γ emission and the high sensitivity of NSPECT to γ rays produces a better image.

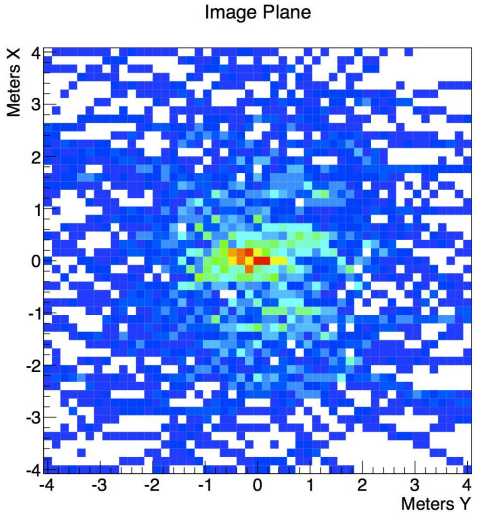

Fig. 18a. Neutron image of a bare ^{252}Cf source.

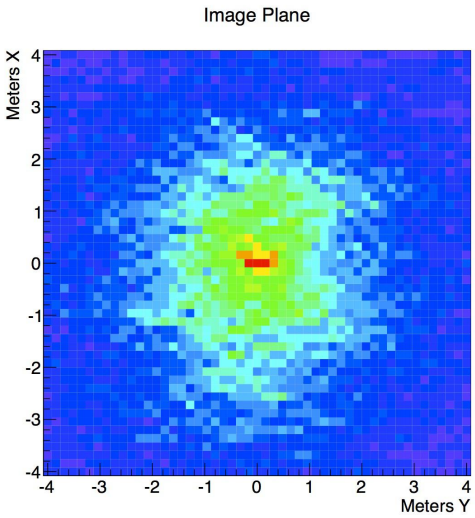

Fig. 18b. γ image of bare ^{252}Cf source.

In Fig. 19 are the corresponding images (neutron and γ) of the same source, but inside the moderating HDPE sphere. The reduced intensity of the neutron source is evident (for the same exposure length) in Fig. 19a, while little attenuation is seen in the γ image (Fig. 19b). The integrated emission is weak enough in Fig. 20a, so that individual event circles are evident. About fifty events are registered, enough for a coherent neutron source identification and location.

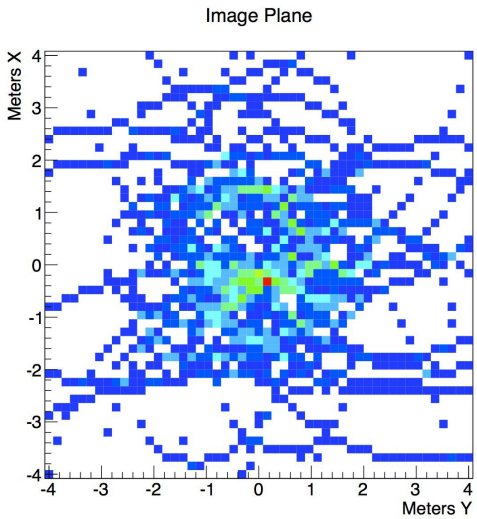

Fig. 19a. Image of moderated neutron source.

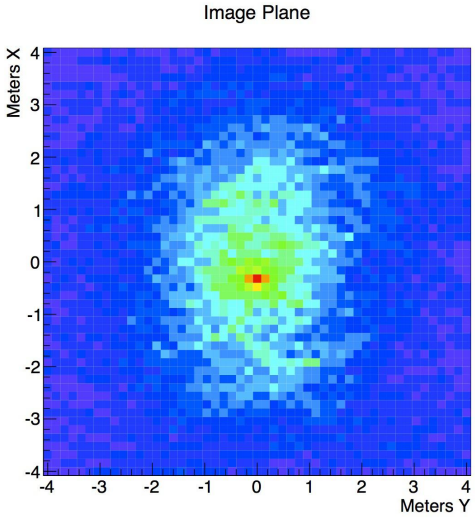

Fig. 19b. γimage of neutron-moderated source.

In Fig. 20a and b are the neutron and γ spectra, both moderated and unmoderated, after selecting events from the image position (slightly lower in elevation than the bare source). The neutron signal is reduced considerably, but the source is still plainly present in the γ signal. The basic exponential form of the Watt spectrum is still apparent, but greatly reduced

in amplitude. No such significant modification of the spectrum or its intensity is seen in the γ signal is seen in Fig. 20b. However, the intensity below about 500 keV is affected but the spectrum is basically unaltered above that.

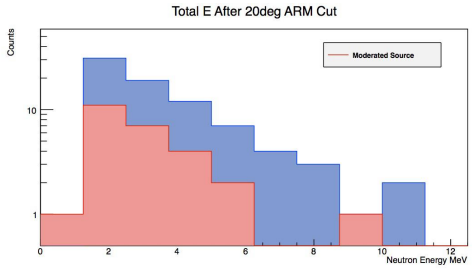

Fig. 20a. Neutron spectra from moderated and unmoderated neutron source.

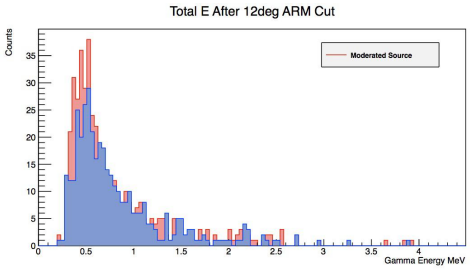

Fig. 20b. γ spectra from the moderated and unmoderated neutron source.

CONCLUSIONS

NSPECT, the neutron spectrometer telescope, a joint venture of Michigan Aerospace Corp. and the University of New Hampshire has been exercised as an operating imaging spectrometer. Its ability to simultaneously image and measure neutrons and γ rays makes is a powerful tool for a variety of domestic forensic and remote sensing radiation situations. Resolution figures for neutron and γ energy and angle are comparable to those taken under ideal conditions for two cells. When fully populated with seventy-seven cells per plane, the instrument efficiency will increase by 9.5× for both neutrons and γ rays.

ACKNOWLEDGMENTS

This work was and is supported by the Defense Threat Reduction Agency through Michigan Aerospace Corp., contracts HDTRA1-08-C-0077 and HDRTA1-11-C-0054. It builds on research started with funding from NNSA NA-22.

REFERENCES

[1] Schönfelder, V. et al., Instrument Description and Performance of the Imaging Gamma-Ray Telescope COMPTEL Aboard the Compton Gamma-Ray Observatory, Ap. J., vol. 86, pp. 657-692, 1993.

[2] Bravar, U.; Woolf, R.S.; Bruillard, P.J.; Flückiger, E.O.; Legere, J.S.; MacKinnon, A.L.; Macri, J.R.; Mallik, P.C.; McConnell, M.L.; Pirard, B.; Ryan, J.M., Calibration of the Fast Neutron Imaging Telescope (FNIT) Prototype Detector, IEEE Trans. Nuc. Sci., vol 56, Issue 5, part 2, pp. 2947-2954, 2009.